5B.3 REGIONAL-SCALE ASPECTS OF THE DIURNAL PRECIPITATION CYCLE

D. A. Ahijevych[1], R. E. Carbone, and C. A. Davis
NCAR[2], Boulder, CO

1 ABSTRACT

National composites of radar reflectivity have permitted fine-scale analysis of the diurnal cycle of precipitation over the U.S. Previous studies focused on thunder observations and rain gage measurements to document favored times of day for precipitation over the U.S. However, these methods lacked the sensitivity, spatial resolution, and blanket coverage that the WSR-88D network provides. More recently, the National Lightning Detection Network (NLDN) and satellite-based optical transient detector (OTD) have produced reasonable pictures of the diurnal climatology of lightning over both land and ocean. While these lightning sensors benefit from extended or even global coverage, the platforms still suffer from their own unique limitations.

On the continental scale, the findings based on the radar network are qualitatively similar to results based on rain gage or thunderstorm observations. However, regional and smaller-scale features observed in the phase and amplitude of the diurnal cycle are not documented in the literature. These features include an apparent lake breeze influence southwest (upwind) of Lake Michigan and Superior, a sea/land breeze signal along the Gulf coast and Atlantic seaboard, and a tendency for rainfall to peak later eastward from the Appalachian Mountains. The latter aspect echoes a better-known pattern seen on a larger scale in the lee of the Rocky Mountains. Systematic phase shifts apparently due to mountain-valley circulations are also evident within the Rocky Mountain cordillera itself. In addition to the diurnal cycle, the geographical distribution of the second harmonic (semi-diurnal) signal is also presented.

2 INTRODUCTION

Due to the rotation of the earth within the earth-sun system, many atmospheric processes are inexorably linked to the diurnal cycle. The periodic forcing pervades a spectrum of spatial scales from planetary pressure waves to local sea breezes. Even noisy fields such as precipitation exhibit a distinct 24-h period given a sufficiently long averaging interval.

The phase and amplitude of this precipitation signal over the U.S. has been studied by past observers using various platforms or proxies for rainfall. For example, Wallace (1975) used hourly precipitation and thunder observations. Others have used regional rain gauge networks (Easterling and Robinson, 1985; Riley et al., 1987; Balling, 1985; Dai et al., 1999). Lightning flash records from the National Lightning Detection Network (Zajac and Rutledge, 2001) and the TRMM Lightning Imaging Sensor (Williams et al., 2000) have also shed light on the distribution of precipitation throughout the day. Additionally, the TRMM Microwave Imager and precipitation radar have enabled diurnal climatologies of tropical rainfall over land (Sorooshian et al., 2002).

Despite its advantages over other platforms, a radar-based climatology of the precipitation diurnal cycle over the U.S. has not been established. Frequent sampling and homogenous coverage make the NOWrad™ product well suited for such an endeavor. Its fine spatial and temporal resolution and sensitivity to moderate and light rainfall distinguish it from conventional rain gauge networks and satellite platforms. While lightning detection networks may offer superior spatial coverage, they do not detect weaker convective elements with no lightning. Warm-rain clouds (above 0C) with very little or no lightning can and often do produce substantial rainfall. Weather radar, on the other hand, both detects and discriminates light, moderate, and heavy precipitation relatively well.

Subsequent sections describe the radar dataset and the methodology, followed by interpretation and summary of the results. Newer, regional-scale aspects of the diurnal climatology are emphasized.

3 DATASET

The foundation of this radar climatology is the NOWrad™ product produced by Weather Systems International (WSI) Corporation. Every 15 min, WSI merges NIDS reflectivity data from individual WSR-88D sites into a single national composite. The merging process is proprietary to WSI, but the final product essentially depicts the highest reflectivity measured vertically above each grid point. The reflectivity is mapped onto a latitude/longitude grid with 2-km spacing and in 5-dBZ increments. Automated WSI computer algorithms filter bad data both from individual sites and from the national composite before a radar meteorologist removes anomalous propagation echoes and other artifacts by hand. For our climatology, we compiled seven complete warm seasons (1996-2002, May through August) of NOWrad™ products with minimal dropout (~1%).

As mentioned earlier, this dataset benefits from exceptional resolution and reliability. Some data is lost however in the mountainous western U.S. where significant beam blockage occurs. In addition, the 5-dBZ granularity precludes any serious quantitative precipitation estimation. Also, the compositing process does not completely remove individual radar biases and patterns of range-dependent detection efficiency. Beam blockage in the west and circular patterns centered on individual WSR-88D radar sites are evident in Fig. 1, the percentage time that radar reflectivity exceeds 15dBZ over any particular point.

4 METHODOLOGY

For expediency, the NOWrad™ products were grouped by the hour. For example, four times were merged to represent 0100 UTC (0045, 0100, 0115, and 0130 UTC). Instead of converting the reflectivity to rainfall rate and averaging the rainfall rates, the final field is the fraction of

[1] NCAR, Boulder, CO, 80307-3000, ahijevyc@ucar.edu
[2] NCAR is sponsored by the National Science Foundation.

time that a reflectivity threshold was met or exceeded at each grid point. When a grid point met or exceeded this threshold, it was recorded as a precipitation event. Over the course of many times, days, and seasons, this produced a smooth field with little impact from any one particular rainfall episode. This methodology ensured that infrequent, but high reflectivity outliers did not skew the results. Occasionally, bad high reflectivity (>65 dBZ) data did propagate to the final NOWrad™ product and could contaminate estimated rainfall rate climatologies. The threshold method minimized this problem while retaining some semblance to rainfall quantity in the final field.

Diurnal variations were analyzed by Fourier decomposition. Essentially, sine curves of varying period were fit to the 24 hourly values using a least-squared-error method. While the discrete Fourier decomposition theoretically produces 12 harmonics down to the 2-hourly period, we only feature the zeroth, first and second components in this study. These correspond to the daily mean, diurnal, and semi-diurnal cycles. In the process, we calculated the amplitude and the time of the occurrence of the maximum in the first harmonic, expressed as a phase angle. Since this amplitude was a function of the mean number of occurrences through the day, it was normalized by dividing it by the daily mean. Using the phase angle of the first harmonic and longitude at each grid point, the time for the peak in the diurnal cycle was converted to local solar time (LST) assuming LST = UTC + longitude(degrees) /15.

5 RESULTS

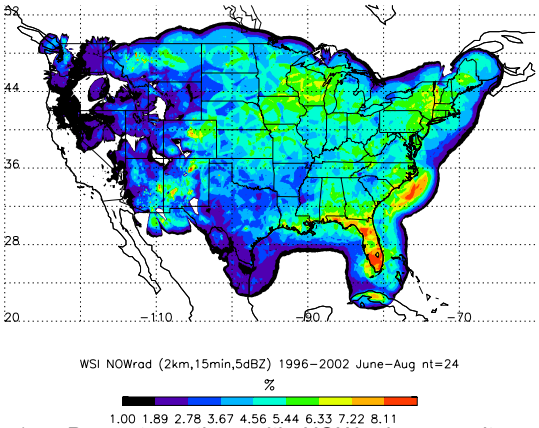

Fig. 1. Percentage time with NOWrad composite radar reflectivity ≥ 15 dBZ for June-August, 1996-2002. This is equivalent to the amplitude of the zeroth harmonic derived from the hourly time series.

The fraction of time radar reflectivity meets or exceeds 15 dBZ is in Fig. 1. This is a very light rain threshold, approximately equivalent to the smallest measurable precipitation rate by a standard NWS rain gage (0.25 mm/h). Precipitation is observed most frequently over Florida and in narrow band at the edge of the observing network 100-200 km offshore from the Carolinas. This oceanic hotspot is most likely attributable to the warm waters of the Gulf Stream. Narrow secondary peaks branch westward and northeastward from Florida along the northern Gulf coast and the Atlantic seaboard. Further inland, away from the sea-breeze regime, precipitation frequency decreases rapidly. However, there are broad peaks in the north-central U.S. (Iowa and Wisconsin) and the Northeast. When the precipitation threshold is increased to 40 dBZ (not shown), the Northeastern maximum disappears, while the north central peak remains (displaced slightly to the southwest), suggesting frequent but less intense rainfall in the Northeast relative to the north-central U.S. Further west, precipitation frequency declines dramatically to near zero in southern California.

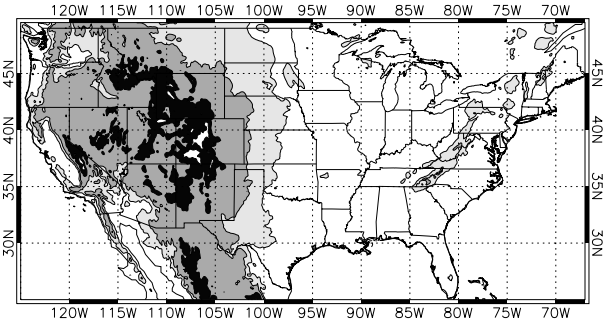

Fig. 2. U.S. state borders and coastlines with surface elevation above mean sea level (AMSL). Contoured at 500, 1000, 2000,and 3000 m with progressively darker shading between 500 and 3000 m. The Rocky Mountains are in the west and the Appalachian Mountains in the east.

In the west, beam blockage dominates the amplitude pattern. For example, note the wedge-shaped spokes of depressed values emanating from the Seattle/Tacoma radar in mountainous Washington State. (For reference, U.S. topography is plotted in Fig. 2.) Other network artifacts manifest themselves as circular bands of enhanced amplitude in the central and north-central U.S. These subtle structures probably stem from radar geometry--the further from a radar site, the higher the lowest beam is above the surface. This makes the detection efficiency a function of range, which manifests itself as overlapping circles in our composite. One must not ascribe meteorological explanations to these artificial amplitude fluctuations. Finally, there are a few suspicious grid points with inflated values towards the perimeter of the network (e.g. Arizona, New Mexico and northern tip of New York state). They occur at WSR-88D sites and are probably due to ground clutter.

The amplitude of the first harmonic based on the hourly time series of fraction of time with reflectivity ≥ 15dBZ is shown in Fig. 3. This is normalized amplitude, comparable to results in Wallace (1975), Easterling and Robinson (1985), Balling (1985), and Dai et al. (1999). It is obtained by dividing the amplitude of the first harmonic by the amplitude of the zeroth harmonic at each grid point. It quantifies the "peakedness" of the hourly time series, ranging from zero for a flat time series to two in the case of all zero values, save one. Most values lie between 0.1 and 1.5 with low values near the Great Lakes, central Mississippi River Valley, and parts of Texas and Oklahoma. The highest values are reserved for the Rocky Mountains, the southeast U.S, the Florida peninsula, and Cuba. As shown by previous investigators, ubiquitous conditional instability across the southeast U.S. supports a strong diurnal cycle in precipitation. Under return flow from the Bermuda High, the Gulf coast plains and Florida peninsula have a steady supply of tropical moisture that is regularly tapped by deep convection initiated along various mesoscale boundaries such as sea breeze fronts and other thunderstorm-induced cold pools. Albeit dryer than the southeast, the mountainous west also experiences a

prominent precipitation diurnal cycle, amplified by the peakedness of the hourly time series. High precipitation frequency is clustered tightly during the early afternoon with little, if any, precipitation falling at night.

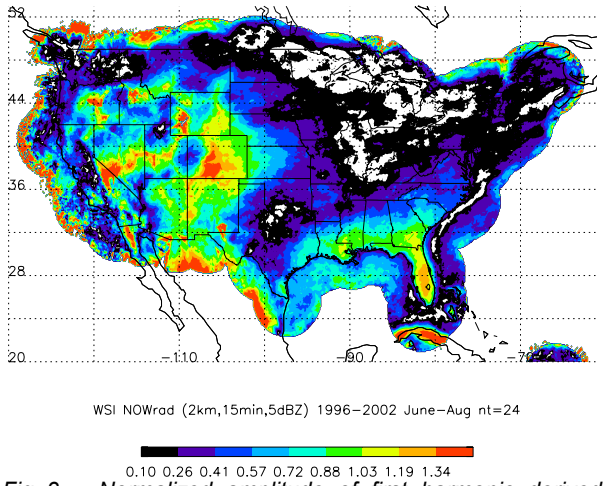

Fig. 3. Normalized amplitude of first harmonic derived from hourly time series of percentage time with radar reflectivity ≥ 15 dBZ for June-August, 1996-2002. The precipitation diurnal cycle is strongest over the higher Rocky Mountains and the southeast U.S. with broad secondary maxima extending into the Great Plains and the Appalachian Mountains.

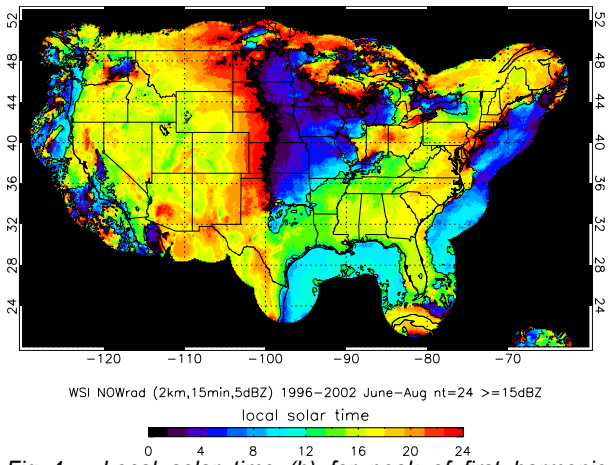

Fig. 4. Local solar time (h) for peak of first harmonic derived from hourly time series of percentage time with radar reflectivity ≥ 15 dBZ for Jun-Aug, 1996-2002.

The time of the diurnal maximum derived from the phase of the first harmonic is shown in Fig. 4. An alternative measure would be the time with the greatest hourly value (as opposed to the time of the peak of the fitted sine curve). For the most part, these two times coincide within 1-2 h.

The land and sea-breeze regimes dominate coastal regions of the northern Gulf of Mexico, Florida, and Georgia. The distribution of phase shifts is distinctly bimodal with early morning (0400-0500 LST) maxima over water and early evening peaks over land (1600-1700 LST).

Other large-scale features in Fig. 4 have been well documented by previous investigators. For example, measurable precipitation is most frequent near the time of maximum cumulative heating (1500-1700 LST) over the higher terrain of the Rocky Mountains. This elevated heat source drives large-scale low-level convergence and ascent over the plateau during the day and descent over the adjacent plains (Reiter and Tang, 1984; Dai et al., 1999). As the solenoid reverses at night, subsidence and convective inhibition diminish over the plains and thunderstorms propagate away from the mountains. These storms often draw strength from a burgeoning nocturnal low-level jet that pumps heat and moisture poleward from the Gulf of Mexico.

There is a smooth transition from an evening to early morning peak across the Great Plains, suggesting afternoon thunderstorms generated over the higher terrain are linked to subsequent rainfall further east. Previous investigators have addressed the question of how much of the early morning maximum is attributed to eastward-propagating storms and how much is ascribed to in-situ generation. Riley et al. (1987) offer, "Many (but not all) of the convective systems die out across western Kansas and Nebraska before sunrise the next morning. Some of the mountain generated convective rainstorms become organized . . . [and] persist for several days." Riley et al. continue, "Our results also reveal, however, that a significant portion of the Plains warm season nocturnal rainfall is locally generated and can not be explained by the simple eastward advection of mountain generated precipitation systems from the previous afternoon." Dai et al. (1999) add, "East of about 97W the nocturnal maximum is much weaker [than over the eastern slopes of the Rockies], and the phase does not change significantly, indicating that most of the eastward propagating thunderstorms die out around 97W." Carbone et al. (2002) analyzed Hovmoller diagrams of warm season precipitation over the U.S., and actually tracked the longitude of individual precipitation events. They uncovered coherent precipitation episodes that frequently initiated near the Rocky Mountains in the early evening and propagated eastward for more than 20 hours.

Although the diurnal amplitude is smaller and the pattern is less pervasive, a similar delayed phase shift pattern is evident between the Appalachian Mountains and Atlantic coast between 36N and 44N. The eastward phase speed of this peak in the diurnal cycle is slower than that observed in the central Great Plains, but its similarity suggests the mountain-plains dynamics responsible for the nocturnal activity in the lee of the Rockies are also present in the lee of the Appalachians. This subtle feature may go unnoticed in courser climatologies based on 2.5 or even 1-degree gridded rain gauge datasets.

In a broad sense, the Rocky Mountains exhibit a uniform early afternoon precipitation maximum. However, fine structure in the phase diagram is correlated to local topography. These phase variations are probably attributable to local mountain-valley circulations that manipulate the preferred initiation time for afternoon thunderstorms.

Another subtle feature of the phase shift field is observed east of Minnesota and northern Wisconsin through the entire Great Lakes region. The convoluted phase pattern is complex and possibly influenced by a number of precipitation regimes. First, there is the land and lake-breeze regime, which features afternoon thunderstorms over land and weaker precipitation over the lake during the night. Then there are remnants of nocturnal thunderstorms that propagate into the region from the Great Plains. Additionally, there is the straightforward continental

regime characterized by short-lived, unorganized thunderstorms fueled by afternoon heating. Admittedly, this phase pattern is diffuse and not so robust, considering the weaker diurnal cycle and wider error bars of the phase calculation. However, a longer climatology may sharpen the picture and help isolate the effects of the Great Lakes on the diurnal cycle of precipitation in adjoining regions.

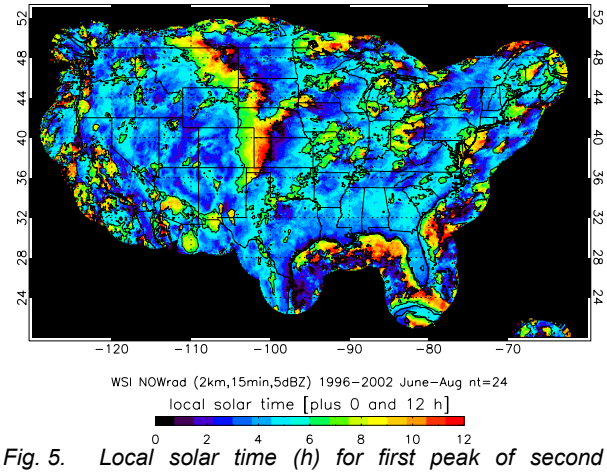

Fig. 5. Local solar time (h) for first peak of second harmonic derived from hourly time series of percentage time with radar reflectivity ≥ 15 dBZ for Jun-Aug, 1996-2002.

The times of the semi-diurnal peaks derived from the second harmonic are shown in Fig. 5. Most of the country experiences the first peak between 0200 and 0500 LST (second peak between 1400 and 1700 LST). Basic tidal theory predicts maximum surface convergence due to the solar semi-diurnal progressive pressure wave at 0700 and 1900 LST. However, there is scant evidence of this forcing mechanism at work in the precipitation observations. The precipitation peaks do not match the theoretical times of maximum surface convergence.

The contribution of the second harmonic to total hourly variance was relatively small. Its contribution was less than 25% for most of the domain, whereas the variance explained by the first harmonic exceeded 75% over most locations (not shown). One should also note that in locations with predominant diurnal peaks, the onset of precipitation is often more sudden than the decline, and the resultant asymmetry about the diurnal peak in the time series adds some power to the semi-diurnal harmonic.

6 SUMMARY

With 2-km reflectivity composites over the U.S., it is possible to examine the diurnal cycle of precipitation in fine spatial detail. While previous studies identified broad features such as the strong diurnal cycle in the Rocky Mountains and the southeast coastal plain, this dataset reveals smaller-scale features such as subtle phase shifts within the Rocky Mountain cordillera itself. Additionally, the shift to nocturnal precipitation east of the Rockies is repeated east of the Appalachians. A weaker, yet broader Great Lakes signal is suggested near Michigan where the smooth progression of the diurnal cycle phase shift east of the Rockies is disrupted. Lastly, over the entire domain, little hourly rainfall variance is explained by the semi-diurnal period.

As numerical models grow more sophisticated in their simulation of the diurnal cycle, it is important to have a good benchmark for comparison. Local knowledge of the diurnal cycle may also aid forecasters in quantitative rainfall prediction, perhaps complimenting numerical model forecasts. Future work will compare the simulated diurnal cycle from the Weather Research Forecast Model (WRF) to the radar observations.

7 REFERENCES

Balling, R. C., Jr., 1985: Warm season nocturnal precipitation in the Great Plains of the United States. *J. Climate Appl. Meteor.*, **24**, 1383-1387.

Carbone, R. E., J. D. Tuttle, D. A. Ahijevych, and S. B. Trier, 2002: Inferences of predictability associated with warm season precipitation episodes. *J. Atmos. Sci.*, **59**, 2033-2056.

Dai, A. D., F. Giorgi, and K. E. Trenberth, 1999: Observed and model-simulated diurnal cycles of precipitation over the contiguous United States. *J. Geophys. Res.,* **104**, 6377-6402.

Easterling, D. R. and P. J. Robinson, 1985: The diurnal variation of thunderstorm activity in the United States. *J. Climate Appl. Meteor.,* **24**, 1048-1058.

Reiter, E. R., and M. Tang, 1984: Plateau effects on diurnal circulation patterns. *Mon. Wea. Rev*., **112**, 638-651.

Riley, G. T., M. G. Landin, and L. F. Bosart, 1987: The diurnal variability of precipitation across the central Rockies and adjacent Great Plains. *Mon. Wea. Rev*., **115**, 1161-1172.

Sorooshian, S., X. Gao, R. A. Maddox, Y. Hong, H. V. Gupta, and B. Imam, 2002: Diurnal variability of tropical rainfall retrieved from combined GOES and TRMM satellite information. *J. Climate*, **15**, 983-1001.

Wallace, J. M., 1975: Diurnal variations in precipitation and thunderstorm frequency over the conterminous United States. *Mon. Wea. Rev*, **103**, 406-419.

Williams, E., K. Rothkin, D. Stevenson, and D. Boccippio, 2000: Global lightning variations caused by changes in thunderstorm flash rate and by changes in the number of thunderstorms. *J. Appl. Meteor*. **39**, 2223-2230.

Zajac, B. A. and S. A. Rutledge, 2001: Cloud-to-Ground Lightning Activity in the Contiguous United States from 1995 to 1999. *Mon. Wea. Rev*., **129**, 999-1019.

8 ACKNOWLEDGEMENTS

This research was sponsored by National Science Foundation support to the U.S. Weather Research Program. Thanks to John Tuttle, Dan Megenhardt, and Jason Knievel for software, inspiration, and constructive comments, and to the Marshall Space Flight Center Global Hydrology Research Center for sharing their archive of WSI NOWrad™ products.